




K_{ATP} channel activity and slow oscillations in pancreatic beta cells are regulated by mitochondrial ATP production

Jeremías Corradi^{1,2} , Benjamin Thompson^{1,2}, Patrick A. Fletcher³ , Richard Bertram⁴, Arthur S. Sherman³ and Leslie S. Satin^{1,2} 

¹Department of Pharmacology, University of Michigan Medical School, Ann Arbor, MI, USA

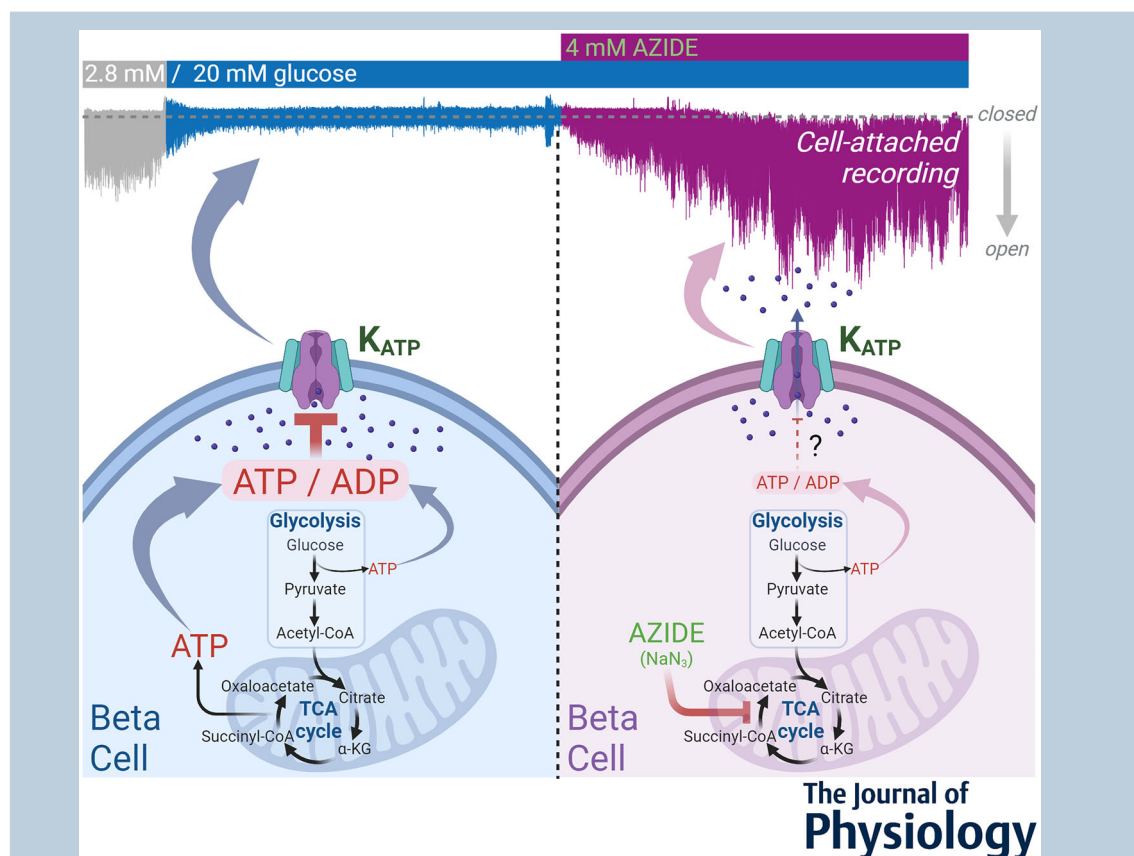
²Brehm Diabetes Research Center, University of Michigan Medical School, Ann Arbor, MI, USA

³Laboratory of Biological Modeling, National Institute of Diabetes, Digestive, and Kidney Diseases, National Institutes of Health, Bethesda, MD, USA

⁴Department of Mathematics and Programs in Neuroscience and Molecular Biophysics, Florida State University, Tallahassee, FL, USA

Handling Editors: Peking Fong & Kyle McCommis

The peer review history is available in the Supporting Information section of this article (<https://doi.org/10.1113/JP284982#support-information-section>).



Abstract Pancreatic beta cells secrete insulin in response to plasma glucose. The ATP-sensitive potassium channel (K_{ATP}) links glucose metabolism to islet electrical activity in these cells by responding to increased cytosolic [ATP]/[ADP]. It was recently proposed that pyruvate kinase (PK) in close proximity to beta cell K_{ATP} locally produces the ATP that inhibits K_{ATP} activity. This proposal was largely based on the observation that applying phosphoenolpyruvate (PEP) and ADP to the cytoplasmic side of excised inside-out patches inhibited K_{ATP}. To test the relative contributions of local vs. mitochondrial ATP production, we recorded K_{ATP} activity using mouse beta cells and INS-1 832/13 cells. In contrast to prior reports, we could not replicate inhibition of K_{ATP} activity by PEP + ADP.

However, when the pH of the PEP solutions was not corrected for the addition of PEP, strong channel inhibition was observed as a result of the well-known action of protons to inhibit K_{ATP} . In cell-attached recordings, perfusing either a PK activator or an inhibitor had little or no effect on K_{ATP} channel closure by glucose, further suggesting that PK is not an important regulator of K_{ATP} . In contrast, addition of mitochondrial inhibitors robustly increased K_{ATP} activity. Finally, by measuring the [ATP]/[ADP] responses to imposed calcium oscillations in mouse beta cells, we found that oxidative phosphorylation could raise [ATP]/[ADP] even when ADP was at its nadir during the burst silent phase, in agreement with our mathematical model. These results indicate that ATP produced by mitochondrial oxidative phosphorylation is the primary controller of K_{ATP} in pancreatic beta cells.

(Received 5 May 2023; accepted after revision 16 October 2023; first published online 17 November 2023)

Corresponding author L. S. Satin: Department of Pharmacology, University of Michigan Medical School, Ann Arbor, Michigan 48105, USA. Email: lsatin@umich.edu.

Abstract figure legend The intracellular mechanisms that control K_{ATP} channel activity in insulin-secreting pancreatic beta cells were investigated. From inside-out and cell-attached electrophysiological recordings, we found that K_{ATP} activity was not significantly affected by ATP synthesized by pyruvate kinase. However, in intact beta cells perfused with high glucose concentrations, we observed a dramatic increase in K_{ATP} channel activity when mitochondrially produced ATP was inhibited by NaN_3 or rotenone (two inhibitors of the electron transport chain). These results confirm that the ATP synthesized by oxidative phosphorylation is the main factor responsible for K_{ATP} modulation in beta cells. This mechanism was also supported by simulations of the Integrated Oscillator Model for beta cells. The top trace in the figure corresponds to a cell-attached recording of K_{ATP} obtained from mouse beta cells under the indicated conditions.

Key points

- Phosphoenolpyruvate (PEP) plus adenosine diphosphate does not inhibit K_{ATP} activity in excised patches. PEP solutions only inhibit K_{ATP} activity if the pH is unbalanced.
- Modulating pyruvate kinase has minimal effects on K_{ATP} activity.
- Mitochondrial inhibition, in contrast, robustly potentiates K_{ATP} activity in cell-attached patches.
- Although the ADP level falls during the silent phase of calcium oscillations, mitochondria can still produce enough ATP via oxidative phosphorylation to close K_{ATP} .
- Mitochondrial oxidative phosphorylation is therefore the main source of the ATP that inhibits the K_{ATP} activity of pancreatic beta cells.

Introduction

ATP-sensitive potassium channels (K_{ATP}) couple increased glucose level with insulin release (Ashcroft & Rorsman, 1989; Cook & Hales, 1984; Nichols, 2006; Rorsman & Trube, 1985). Many observations have supported this view: K_{ATP} is the dominant resting conductance of the beta cell (Ashcroft & Rorsman, 1989;

Nichols, 2006; Satin et al., 2015), mutations in the channel are strongly linked to metabolic diseases (Ashcroft et al., 2017; Pipatpolkai et al., 2020) and drugs targeting K_{ATP} are oral anti-diabetic agents (Ashcroft et al., 2017). K_{ATP} is the main link connecting glucose metabolism to the membrane depolarization that activates voltage-gated calcium channels. This increases the intracellular calcium concentration, which in turn evokes the release of insulin

Jeremías Corradi is an Assistant Professor of Pharmacology at the National University of the South, in Argentina, where he carried out his PhD and postdoctoral studies with Cecilia Bouzat. His research has utilized patch clamp and computational techniques to study ligand-gated ion channels. He is currently a postdoctoral fellow in the Department of Pharmacology at the University of Michigan. **Les Satin** is Professor of Pharmacology at Michigan. After obtaining his PhD at UCLA, he carried out postdoctoral work with Paul Adams at Stony Brook and Dan Cook at the University of Washington. His work focuses on islet ion channels, cell fuel metabolism, calcium signalling and diabetes.



(Nichols, 2006). K_{ATP} is spontaneously active, and its activity is directly blocked by ATP and increased by ADP, as shown by recordings of channel activity in inside-out membrane patches (Bokvist et al., 1991; Cook & Hales, 1984; Rorsman & Trube, 1985). Therefore, the cytosolic ratio of ATP and ADP concentrations (referred to as $[ATP]/[ADP]$) is an important regulator of K_{ATP} activity and, by extension, of calcium oscillations and insulin release. Furthermore, as we have recently shown, oscillations in K_{ATP} drive oscillations in islet electrical activity (Marinelli et al., 2022).

Although the high density of mitochondria present in beta cells (Kaufman et al., 2015; Rutter et al., 2023; Wang et al., 2021) and the efficient production of ATP by oxidative phosphorylation make mitochondrially derived ATP a probable candidate as the source of ATP that closes K_{ATP} physiologically, this has been challenged recently by the finding that, in excised membrane patches from beta cells, application of the glycolytic intermediate phosphoenolpyruvate (PEP) in the continuous presence of ADP leads to channel closure (Foster et al., 2022; Lewandowski et al., 2020). The reports proposed that a local pool of ATP at the plasmalemma is responsible for K_{ATP} closure and is produced by glycolytic enzymes such as pyruvate kinase (PK) co-localized with K_{ATP} (Foster et al., 2022; Lewandowski et al., 2020). Based on these observations, it was suggested that local rather than bulk or mitochondrially derived ATP closes the channel, triggering cell depolarization, calcium influx and insulin secretion from beta cells. Furthermore, mutations in particular PK isoforms were subsequently shown to alter islet calcium signalling and secretion, although the phenotypes observed in PK knockout mice were mild (Foster et al., 2022).

To evaluate this hypothesis, we recorded the activity of single K_{ATP} channels from mouse beta cells and INS-1 832/13 cells in two different electrophysiological configurations: inside-out and cell-attached patches. Using inside-out recordings, we were unable to reproduce the reported inhibition of K_{ATP} activity by ADP and PEP applied to the cytoplasmic face of the membrane. However, an inhibitory effect of PEP solutions was observed when the pH was not corrected, confirming that PEP can inhibit K_{ATP} channels as a result of protons, a well-known mechanism (Fan et al., 1994; Mislser et al., 1989; Proks et al., 1994). These and other findings from our inside-out patch experiments thus fail to support the hypothesis that local glycolysis controls K_{ATP} activity in beta cells.

Another key pillar of the local glycolytic hypothesis is the assumption that mitochondrial oxidative phosphorylation (OxPhos) is shut off during the silent phase of beta-cell oscillations because of ADP deprivation and therefore cannot be solely responsible for OxPhos driven calcium oscillations (Foster et al., 2022; Merrins

et al., 2022). To test this hypothesis, we mimicked the free running oscillatory activity of islets normally observed in saline containing 11 mM glucose at the same time as measuring dynamic changes in $[ATP]/[ADP]$ in mouse islets expressing percreval-HR. In contrast to the local glycolytic hypothesis, we found that OxPhos remains active throughout the beta cell oscillatory cycle.

Thus, the two sets of experiments presented here support mitochondria, and not glycolysis, as the main physiological source of ATP that regulates K_{ATP} activity and calcium oscillations in beta cells. Further support was provided by simulations of the data using the Integrated Oscillation Model (IOM) (Bertram et al., 2018).

Methods

Ethical approval

To ensure the humane treatment and responsible and judicious use of animals, all experimental procedures of the present study were performed under the regulation and supervision of The Institutional Animal Care & Use Committee (IACUC) of the University of Michigan (protocol PRO00011164). Swiss Webster mice were purchased from Charles River Laboratory (Raleigh, NC, USA) and maintained under a 12:12 h light/dark photoperiod at 20–24°C with food and water available *ad libitum*. Mice aged ~3 months and weighing 25–35 g were killed by CO₂ asphyxiation followed by cervical dislocation, and the pancreas was removed to isolate the islets.

Chemical compounds

ATP, ADP (Cayman Chemical Company, Ann Arbor, MI, USA) and PEP (phosphoenolpyruvate monopotassium salt; P7127; Sigma-Aldrich, St Louis, MO, USA) solutions were freshly prepared on the day of the experiments. PKa (TEPP-46; #505 487; EMD Millipore, Burlington, MA, USA), PKi (PKM2-IN-1; HY-103 617; MedChemExpress, Monmouth Junction, NJ, USA), rotenone (R8875; Sigma-Aldrich) and NaN₃ (Sodium azide; S2002; Sigma-Aldrich) were prepared from frozen stock solutions.

Mouse pancreatic islets isolation

Mouse islets were isolated using previously described methods (Merrins et al., 2016). Briefly, Swiss Webster mice aged ~3 months and weighing 25–35 g were killed by CO₂ asphyxiation followed by cervical dislocation and, after pancreas removal and collagenase digestion, islets from a given mouse were isolated by hand-picking and cultured in standard RPMI 1640 medium containing

11 mM glucose, 10% fetal bovine serum, 10 mM HEPES, 1% penicillin/streptomycin and 1% sodium pyruvate.

Cell culture

INS-1 832/13 cells were grown in RPMI 1640 medium containing 11 mM glucose, 10% fetal bovine serum, 1% penicillin/streptomycin, 10 mM HEPES and 1% sodium pyruvate. Cells were grown in 10 cm culture dishes at 37°C in a 5% CO₂ humidified atmosphere.

Electrophysiology

Patch clamp electrodes were pulled in a horizontal puller (P-97; Sutter Instruments, Novato, CA, USA) from borosilicate glass capillaries (Warner Instruments, Hamden, CT, USA), coated with sylgard (Dow Corning, Midland, MI, USA) and fire polished in a microforge (MF-830; Narishige, Tokyo, Japan) up to a final tip resistance of 5–10 MΩ. Single-channel events were recorded from cells in intact mouse islets or INS-1 832/13 cells in the cell-attached or inside-out configurations at room temperature (20–24°C). One patch was studied per islet. The pipette solution contained (in mM): 140 KCl, 2 MgCl₂, 2 CaCl₂ and 10 HEPES, pH 7.2, adjusted with KOH. For both configurations seals having resistances >2 GΩ were obtained in regular bath solution containing (in mM): 140 NaCl, 3 CaCl₂, 5 KCl, 2 MgCl₂, 10 HEPES, and 0 or 2.8 glucose, pH 7.2, adjusted with NaOH. Single-channel activity in the cell-attached configuration were recorded at 0 mV of holding potential immediately after the giga-seals were established.

For inside-out recordings, the bath solution was changed to a solution containing (in mM): 140 KCl, 2 MgCl₂, 1 EGTA and 10 HEPES, pH 7.2, adjusted with KOH (BS-1) (Cook & Hales, 1984). Some inside-out experiments were recorded using different pipette and bath solutions to match those reported in (Lewandowski et al., 2020). For these experiments the pipette solution contained (in mM): 130 KCl, 2 CaCl₂, 10 EGTA, 10 sucrose and 20 HEPES, pH 7.2, adjusted with KOH. The bath solution contained (in mM): 130 KCl, 2 CaCl₂, 10 EGTA, 0.9 free Mg²⁺, 10 sucrose and 20 HEPES, pH 7.2, adjusted with KOH (BS-2). The free Mg²⁺ concentration was calculated using the WEBMAXC server (<https://somapp.ucdmc.ucdavis.edu/pharmacology/bers/maxchelator/webmaxc/webmaxcE.htm>) and was held constant in every solution that was prepared in BS-2. ATP, ADP and PEP solutions were prepared in either BS-1 or BS-2, and pH was adjusted to 7.2 with KOH, unless otherwise indicated. After a giga-seal was obtained and the bath solution was replaced, patches were pulled off of the cell to obtain the inside-out configuration, and

single-channel activity was recorded at a holding potential of –50 mV.

Channel activity was low-pass filtered at 2 kHz and then digitized at 20 kHz using an EPC-10 USB amplifier (HEKA Instruments, Westfield, MA, USA). Single-channel openings were idealized by the half amplitude threshold criterion using QuB, version 2.0.0.28 (www.qub.buffalo.edu) using a digital low-pass filter with an f_c of 2 kHz. After single-channel recordings were made, channel openings were idealized, and the open-time durations were estimated using the maximal interval likelihood function in QuB with a dead time of 0.1 ms. NP_o corresponds to the open channel probability of more than one channel calculated from 50 s segments collected from each experimental condition, where N is the number of channels in the patch and P_o is the open probability of a single channel. NP_o was expressed as $NP_o = I/i$, and calculated by measuring the total current that flows through the open channels (I), obtained from the event amplitude histogram created with QuB, and the amplitude of the unitary current (i) (Yakubovich et al., 2009). NP_o determined for each experimental condition was expressed as relative to that obtained with 0.1 mM ATP + 0.5 mM ADP (referred to for brevity as ADP below) from the same recording.

[ATP/ADP] measurement

The ratio of ATP to ADP concentrations (referred to as [ATP]/[ADP]) was monitored in the cytosol of islet beta cells using perceval-HR, a genetically encoded fluoroprotein sensor that changes its fluorescence in response to changes in [ATP]/[ADP] (Marinelli et al., 2022; Tantama et al., 2013). Adenoviral delivery was used to transiently express the probe in mouse islets, as described in Merrins et al. (2016).

Statistical analysis

Data are expressed as the mean ± SD, unless otherwise specified, and differences between two or more groups were analysed using one-way analysis of variance (Prism, version 9; GraphPad Software Inc., San Diego, CA, USA) with *post hoc* multiple comparison by Tukey's procedure. $P < 0.05$ was considered statistically significant.

Mathematical modelling

The IOM was simulated using the ode15s function in Matlab 2022b (The MathWorks Inc., Natick, MA, USA). The program code defining the model in both Matlab and xppaut (<https://sites.pitt.edu/~phase/bard/bardware/xpp/xpp.html>) compatible files are included in the Supporting

information (File S1) and are posted at Figshare <https://doi.org/10.6084/m9.figshare.24545830>.

Results

PEP does not reduce K_{ATP} activity in excised patches

To test the hypothesis that glycolytically generated local ATP can close nearby K_{ATP} , we recorded single-channel activity from mouse beta cells and insulin-secreting INS-1 832/13 cells using the patch clamp technique in the inside-out configuration (see Methods). We initially recorded channel activity using pipette and bath solutions that closely matched those previously reported (BS-1), similar to Cook & Hales (1984).

After excising membrane patches from mouse beta cells, single-channel openings were observed as downward deflections of ~ 3 pA (at a holding potential of -50 mV) that had a mean open time of ~ 2.2 ms (Fig. 1A and B). These events were confirmed as corresponding to K_{ATP} activity because they were reversibly inhibited by exposing the cytoplasmic face of the patches to a solution containing 1 mM ATP, observed as a dramatic reduction in NP_o (where N is number of channels and P_o is open probability) and the channel open-time duration (Fig. 1A and B). During patch exposure to the ATP solution, channel activity mainly appeared as isolated events of ~ 1 ms ($P = 0.0057$) with $\sim 90\%$ reduction in NP_o ($P = 0.0016$) compared to that observed under ADP perfusion (Fig. 1B). Switching to a solution containing 0.1 mM ATP and 0.5 mM ADP (referred to as ADP below) provoked strong channel reactivation consisting of events of ~ 2.2 ms grouped into long bursts. The NP_o corresponding to this condition was considered to reflect maximal channel activity, and all other NP_o values are given relative to this (see Methods).

When 5 mM PEP was applied in combination with ADP, no inhibition of K_{ATP} channel activity was apparent, even after 5 min of continuous perfusion of ADP + PEP (Fig. 1A). Channel activity was almost identical to that observed in the presence of ADP alone (Fig. 1A and B), with similar NP_o ($P = 0.633$) and open-time durations ($P = 0.999$, $n = 4$ islets from two mice) (Fig. 1B). Similar results were observed from INS-1 832/13 cells (Fig. 1C and D), with a clear reduction in NP_o ($P < 0.0001$) and open-time duration ($P < 0.0001$) after 1 mM ATP perfusion (Fig. 1D) but no effect when perfusing ADP + PEP ($P = 0.783$ for NP_o and $P = 0.662$ for open-time duration, $n = 10$).

Three PK isoenzymes are expressed in beta cells: PKM1, PKM2 and PKL (DiGrucio et al., 2016; Mitok et al., 2018). Although PKM1 is a tetramer that is constitutively active,

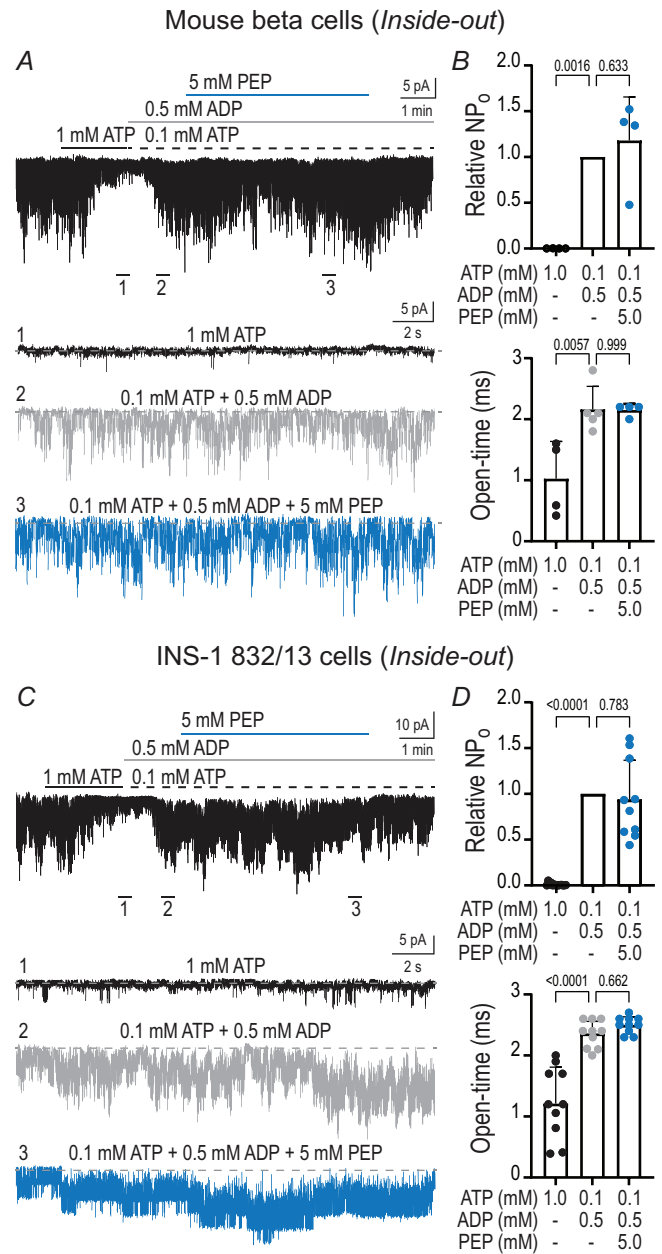


Figure 1. K_{ATP} activity is not affected by PEP in the continuous presence of ADP

K_{ATP} activity evaluated in the presence of the different modulators from mouse beta cells (A and B, $n = 4$ islets from two mice) and INS-1 832/13 cells (C and D, $n = 10$). Single-channel activity was obtained in the inside-out configuration at -50 mV of holding potential. Sections indicated with numbers (1 to 3) from each top trace in (A) and (C) are shown at an expanded time resolution. Channel openings are shown as downward deflections and the dashed lines represent the baseline (zero current). The effect of perfusion of the different compounds was quantified as NP_o and open-time duration (B and D). Values are shown as the mean \pm SD, with P values indicated.

PKM2 and PKL exist as dimeric structures that need to be allosterically converted to their tetrameric forms to be active (Prakasam & Bamezai, 2018; Zhang et al., 2019).

To evaluate if a PK isoform closely associated with the membrane needs to be allosterically activated, we next tested whether TEPP-46 (referred to here as PKa), an activator of the PKM2 isoform (Anastasiou et al., 2012), could reveal the inhibitory effect of PEP on K_{ATP} reported by Lewandowski et al. (2020). K_{ATP} activity was again monitored in inside-out patches excised from INS-1 832/13 cells. Patches were then acutely perfused with ADP + PEP solutions in the presence of 10 μ M PKa, or after a preincubation period (Fig. 2A). Under these experimental conditions, channel activity was again unaffected by PEP and the further addition of PKa had no apparent potentiating effect ($n = 5$) (Fig. 2A and B).

In summary, we were unable to confirm modulation of K_{ATP} activity by PK in inside-out patches.

PEP addition can inhibit K_{ATP} if solution pH is not corrected

PEP is a monocarboxylic acid that is almost fully deprotonated when dissolved in water. When 5 mM

PEP was prepared in BS-1 (see Methods), the solution pH was reduced to pH 4.0. Using the PEP solution of Lewandowski et al. (2020), the pH of the solution was 5.5.

Because protons strongly inhibit K_{ATP} (Allard et al., 1995; Misler et al., 1989; Proks et al., 1994; Xu et al., 2001), we recorded single- K_{ATP} activity in inside-out patches by perfusing ADP + PEP with and without pH correction (Fig. 3). Similar to that shown in Fig. 1, ADP + 5 mM PEP did not inhibit K_{ATP} when the solution pH was buffered (Fig. 3A) because channel activity was almost identical to that observed in the presence of ADP alone (Fig. 3B), with similar NP_o ($P = 0.146$) and open-time durations ($P > 0.999$, $n = 9$ islets from three mice) (Fig. 3C). However, using PEP solutions without a pH correction inhibited K_{ATP} (5 mM PEP, pH 5.5) (Fig. 3A and C), observed as a reduction in NP_o ($P = 0.0002$) and open channel duration ($P < 0.0001$, $n = 8$ islets from two mice) (Fig. 3C). Similar results were observed from INS-1 832/13 cells ($n = 8$) (Fig. 3D–F). Identical results were obtained in mouse beta cells and INS-1 832/13 cells using BS-1 (data not shown).

In a total of 35 excised membrane patches containing K_{ATP} , we never observed K_{ATP} inhibition by ADP + PEP once pH was adjusted to 7.2. Thus, PEP solutions only inhibited K_{ATP} activity in excised patches when pH was uncorrected. Importantly, the pH effect was a result of PEP alone because the addition of ADP to the PEP solutions when pH was unbalanced made no difference to the degree of inhibition seen (data not shown).

Mitochondrial oxidative phosphorylation is the main mechanism controlling K_{ATP} activity in mouse beta cells

We next evaluated K_{ATP} activity in cell-attached patches made using mouse beta cells (see Methods), a more intact model system than the excised patches used above. Cell-attached patches preserve the physiological characteristics of the beta cell, more than excised inside-out patches (Rorsman & Ashcroft, 2018).

K_{ATP} were identified in cell-attached recordings by their characteristic gating pattern and sensitivity to the glucose concentration of the bath solution (Fig. 4). K_{ATP} activity was clearly observed at low bath glucose concentrations, and raising the glucose concentration led to a dramatic reduction in K_{ATP} open probability and the expected appearance of biphasic deflections originating from K_{ATP} closure-induced action potentials (Fig. 4) (Ashcroft et al., 1984; Larsson et al., 1996; Rorsman & Trube, 1985). During perfusion with a 2.8 mM glucose solution, the addition of 10 μ M PKa did not result in any significant reduction in NP_o ($P > 0.999$, $n = 6$ islets from one mouse) (Fig. 4A and B). By contrast, switching to a bath solution containing 20 mM glucose caused a 95% reduction in NP_o

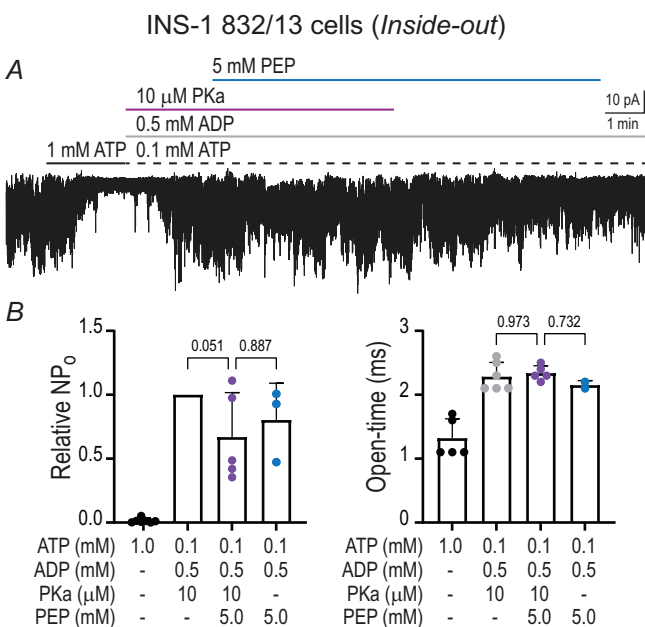


Figure 2. K_{ATP} is not inhibited by ADP + PEP even in the continuous presence of a PK activator

K_{ATP} activity obtained in the presence of PEP and ADP with and without addition of the PK activator TEPP-46 (PKa). A, single-channel events obtained in the inside-out configuration from INS-1 832/13 cells ($n = 5$). B, NP_o and open-time duration from different recordings obtained under the same experimental condition as in (A). Holding potential, -50 mV. Values are shown as the mean \pm SD, with P values indicated.

with respect to that observed in 2.8 mM glucose. To test whether this reduction in channel activity was due to a PK isoform that is closely associated with the membrane, we perfused PKM2-IN-1 (PKi), a PK inhibitor for which the IC_{50} values for the different PK isoforms are $\sim 17 \mu M$ for PKM1, $\sim 3 \mu M$ for PKM2 and $\sim 8 \mu M$ for PKL (Ning et al., 2017). The combined perfusion of 20 mM glucose with $10 \mu M$ PKi failed to significantly change K_{ATP} activity compared to the activity observed in the presence of 20 mM glucose alone: $P > 0.999$, $n = 6$ islets from one mouse (Fig. 4A and B); $P = 0.931$, $n = 4$ islets from two mice (Fig. 4C and D); and $P > 0.999$, $n = 2$ islets from one mouse (Fig. 4E and F). These results are consistent with the conclusion that PK is not an important regulator of K_{ATP} in cell-attached patches, and by extension in intact beta cells.

In contrast, K_{ATP} channels measured in cell-attached patches were robustly and reproducibly activated by

the addition of sodium azide (NaN_3), an inhibitor of mitochondrial cytochrome a_3 (Larsson et al., 1996; Mislser et al., 1989). After reducing K_{ATP} activity by raising the bath glucose concentration to 20 mM, the addition of 4 mM NaN_3 provoked a rapid and dramatic reactivation of K_{ATP} , observed as a ~ 33 -fold increase in NP_o with respect to its value at 20 mM glucose ($P < 0.0001$, $n = 8$ islets from two mice) (Fig. 4C and D). A similar level of K_{ATP} reactivation was observed when NaN_3 was perfused in the presence of $10 \mu M$ PKa, resulting in a ~ 44 -fold increase in NP_o ($P < 0.0001$, $n = 8$ islets from two mice) (Fig. 4C and D). The effect of NaN_3 was mimicked by rotenone, another mitochondrial inhibitor (Chan et al., 2005) ($P = 0.998$ for 20 mM glucose + $0.2 \mu M$ rotenone with and without PKa, $n = 2$ islets from one mouse) (Fig. 4E and F). To confirm that the increase in channel activity we observed was not due to a direct effect of NaN_3 on K_{ATP} , we again recorded K_{ATP} activity in excised patches ($n = 3$ islets from two

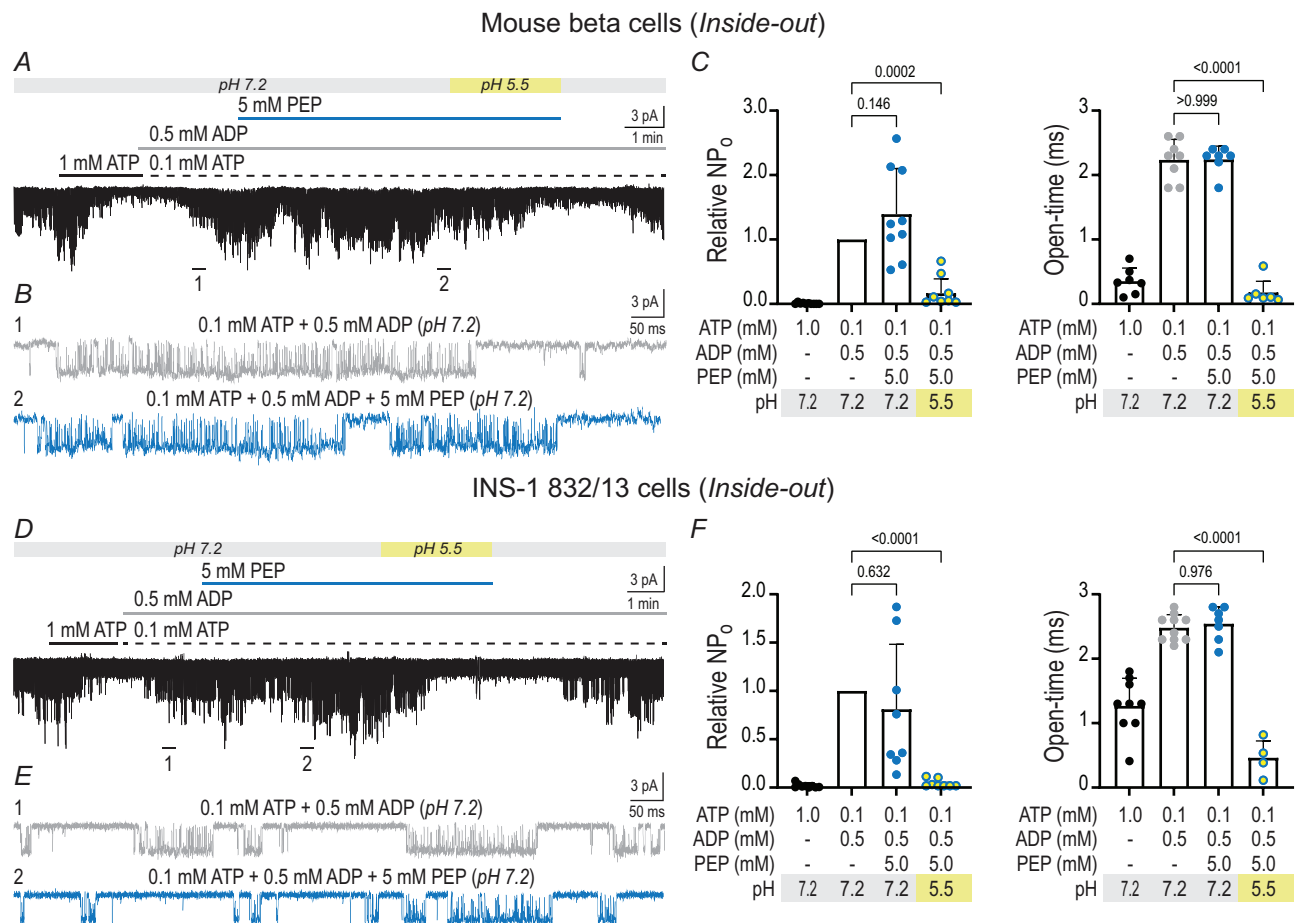


Figure 3. The reduction in pH provoked by PEP is responsible for K_{ATP} inhibition
 K_{ATP} modulation by perfusing PEP in combination with ADP prepared with BS-2 with and without pH correction. PEP solutions showed a pH of 5.5 when prepared at 5 mM concentration and K_{ATP} inhibition was not observed when pH was adjusted to 7.2 (A, from $n = 9$ islets from three mice, and D, from $n = 8$ INS-1 832/13 cells). Sections indicated with numbers (1 and 2) from each top trace in (A) and (D) are shown at an expanded time resolution (B and E). C and F, NP_o and open-time duration obtained from the corresponding single-channel recordings. Holding potential, -50 mV. Values are shown as the mean \pm SD, with P values indicated.

mice) and confirmed that the addition of 4 mM NaN₃ did not directly modulate channel activity (data not shown).

The robustness and reproducibility of NaN₃ or rotenone action to open K_{ATP} in cell-attached but not excised patches contrasted sharply with the weak actions of the PK modulators that we tested in the present study and provide further support for the consensus model in which mitochondrial regulation of the [ATP]/[ADP] ratio indeed predominates in intact beta cells. The access of the two PK modulators into beta cells was confirmed by measuring intracellular Ca²⁺ oscillations in mouse islets

loaded with fura2-AM during continuous perfusion of 11 mM glucose in the absence or the presence of 10 μM PKa or 10 μM PKi (data not shown).

Mitochondrial oxidative phosphorylation is active during the islet silent phase

In addition to experiments with PEP, the local glycolysis hypothesis rests on the assumption that ADP decreases so much during the silent phase of each oscillatory burst that mitochondrial OxPhos is unable to generate sufficient ATP to trigger the next active phase of the oscillation. Instead, it was proposed that the required ATP is produced by pyruvate kinase (Foster et al., 2022; Lewandowski et al., 2020).

Using the IOM (Bertram et al., 2018; Merrins et al., 2016), we simulated a protocol designed to isolate ATP consumption from ATP production at the same time as removing the complexity introduced by spontaneous bursting activity. We set glucose to 11 mM and simulated the effect of diazoxide by reducing the K_{ATP} affinity for ATP, then simulated two 5 min pulses of KCl to mimic burst active phases. The model assumes that ATP is mainly synthesized by mitochondrial OxPhos and that [ATP]/[ADP] drops during the KCl pulses because of calcium-influx induced ATP consumption and a concomitant ADP rise produced by plasmalemmal calcium ATPases (Marinelli et al., 2021, 2022). As can be seen in Fig. 5A, [ATP]/[ADP] recovers during the silent phase because OxPhos continues. Following the second KCl pulse, we simulated the suppression of OxPhos by NaN₃, which shows that [ATP]/[ADP] is predicted by the model to fall in response to the poison even during the silent phase, as expected if OxPhos is still on during this period, and not fully off as predicted in Merrins et al. (2022).

To test the model predictions, we used islets expressing the [ATP]/[ADP] sensor perceval-HR in their beta cells (Marinelli et al., 2022; Merrins et al., 2016; Tantama et al., 2013) (Fig. 5B). We applied two 5 min square pulses of 30 mM KCl in the continual presence of 200 μM diazoxide. To probe for OxPhos activation, we applied 10 mM NaN₃ after the second KCl test pulse. At this dose, NaN₃ rapidly and reversibly reduces [ATP]/[ADP], as confirmed in previous experiments (Marinelli et al., 2022). As shown in Fig. 5B, once the pulse of KCl was applied to mimic the active phase of calcium entry, [ATP]/[ADP] dropped (Marinelli et al., 2022). When KCl was removed to mimic a silent phase, [ATP]/[ADP] recovered. Repeating the KCl pulse application to mimic a second burst active phase again resulted in a clear drop in [ATP]/[ADP]. However, when we restored KCl to 5 mM to mimic a silent phase but added NaN₃ at the same time, [ATP]/[ADP] did not recover and actually fell below the

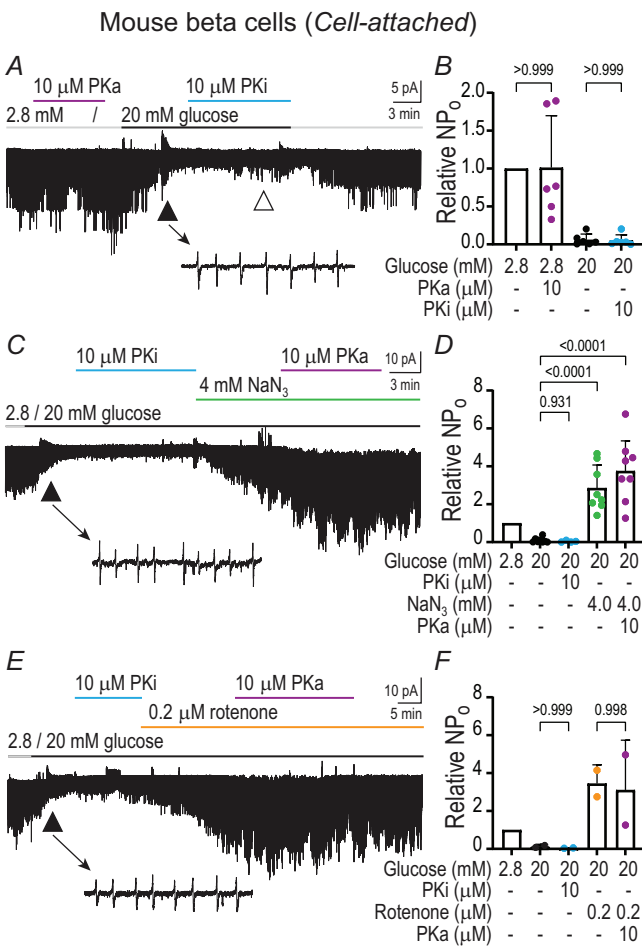


Figure 4. ATP derived from mitochondrial oxidative phosphorylation is the main mechanism that modulate K_{ATP} activity in intact beta cells

K_{ATP} activity from mouse beta cells recorded in cell-attached configuration at a 0 mV holding potential. Activity obtained at 2.8 and 20 mM glucose in the absence and the presence of 10 μM of the different PK modulators (A–F) and in combination of 4 mM NaN₃ (C and D, n = 8 islets from two mice) or 0.2 μM rotenone (E and F, n = 2 islets from one mouse). Biphasic current deflections corresponding to action potentials were observed during 20 mM glucose perfusion (black triangles and inset). Channel reactivation during PKi application (white triangle). Event frequency expressed as NP₀ relative to that observed at 2.8 mM glucose (B, D and F). Values are shown as the mean ± SD, with P values indicated.

level observed during the previous active phase. Washing off NaN_3 resulted in the full restoration of $[\text{ATP}]/[\text{ADP}]$ after several minutes. These results agree with the model predictions in Fig. 5A, indicating that OxPhos contributes substantially to $[\text{ATP}]/[\text{ADP}]$ between the KCl pulses.

These results were observed in 21 islets obtained from a total of four mice. They strongly refute the hypothesis that OxPhos is disabled during the burst silent phases and are in support of the consensus model of islet stimulus-secretion coupling and oscillatory secretion.

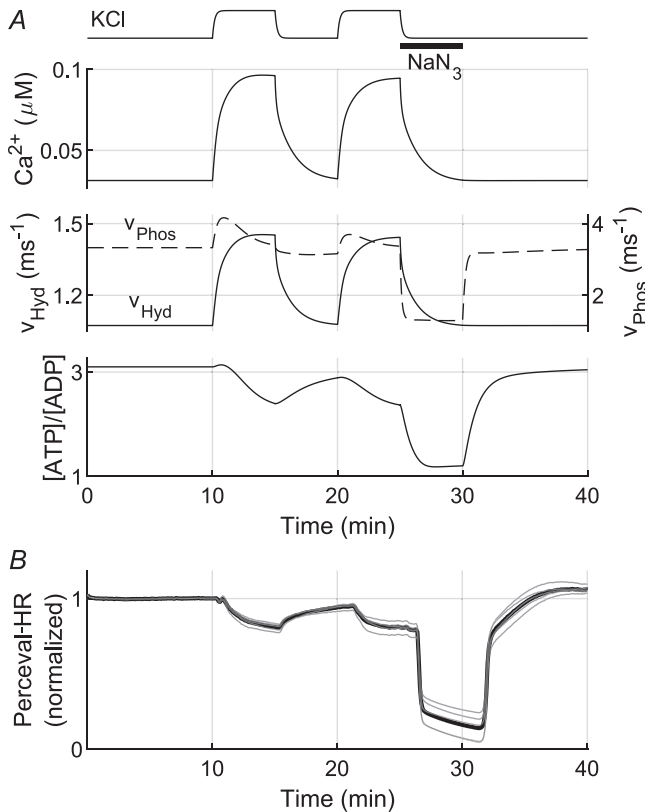


Figure 5. Mitochondrial oxidative phosphorylation is active during the silent phase of bursting in mouse beta cells

A, simulation of the integrated oscillator model (IOM) in 11 mM glucose, under conditions that mimic the application of diazoxide (increasing model parameter k_{tt} from 1 to 4). A series of pulses of KCl are applied by increasing extracellular potassium, model parameter K_o from 5 mM to 10 mM, causing increases in calcium influx and ATP hydrolysis rate (v_{Hyd}) as a result of calcium ATPases. The rate of OxPhos (v_{Phos}) remains relatively unaffected, and so $[\text{ATP}]/[\text{ADP}]$ recovers between pulses, leading to oscillations that mimic bursting. After the second pulse, NaN_3 is simulated (reduction of the model parameter r from 1 to 0.1) causing a dramatic drop in v_{Phos} and consequently in $[\text{ATP}]/[\text{ADP}]$. B, a representative recording of $[\text{ATP}]/[\text{ADP}]$ measured with perceval-HR from five intact mouse islets under the conditions indicated, as were simulated in (A). Detrending was done via linear fit to the first 10 min of the recording, then traces were normalized to the mean ratio calculated from the same initial time interval. The responses of five islets are shown as light grey curves, and the mean across islets in black. The recording is representative of 21 islets obtained from four mice.

To demonstrate the connection between the above pulsed KCl protocol and spontaneous bursting, we used the IOM to simulate spontaneous bursting at 11 mM glucose (Fig. 6A). During burst active phases, calcium rises and causes increased ATP hydrolysis, and the continued ATP production as a result of glycolysis and OxPhos allows recovery of ATP during the silent phases when calcium drops, as described above. The result is a characteristic sawtooth-shaped oscillation in $[\text{ATP}]/[\text{ADP}]$, as has been previously reported (Lewandowski et al., 2020; Li et al., 2013; Marinelli et al., 2022; Merrins et al., 2016). The levels of $[\text{ATP}]/[\text{ADP}]$

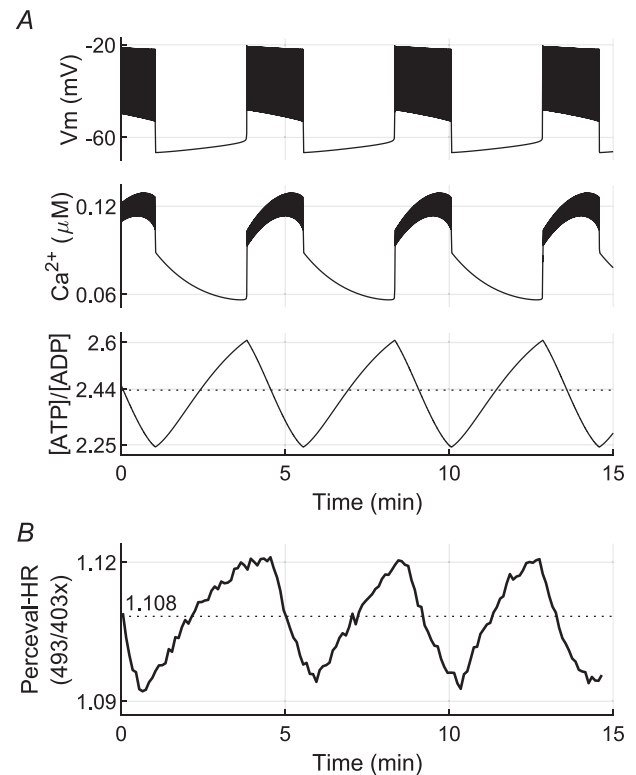


Figure 6. ATP production and consumption during spontaneous bursting

A, simulation of spontaneous bursting in the presence of 11 mM glucose using the IOM model. During burst active phases, increases in calcium drive declines in $[\text{ATP}]/[\text{ADP}]$ ratio as a result of calcium ATPases, whereas, during silent phases, $[\text{ATP}]/[\text{ADP}]$ recovers as a result of continued ATP production. The horizontal dotted line indicates the mean $[\text{ATP}]/[\text{ADP}]$ ratio across three complete periods computed using findpeaks from Matlab Signal Processing Toolbox ($[\text{ATP}]/[\text{ADP}] = 2.4366$). The mean of active phases alone (2.4365) and silent phases alone (2.4423) were very close to this value. B, perceval-HR recording in 11 mM glucose showing oscillations similar to those predicted by the model, with rises and declines during the silent and active phases, respectively. The trace is detrended via linear fit to the whole recording and is representative of more than 40 islets obtained from 10 mice. The horizontal dotted line indicates the mean $[\text{ATP}]/[\text{ADP}]$ ratio across three complete periods (1.1083). As in (A), the mean of active phases alone (1.1053) and silent phases alone (1.1098) were very close to this value.

reached during these oscillations were similar to those observed in Fig. 5A during KCl pulses, with a mean value during the active and silent phases very close to the mean value over three complete periods (Fig. 6A, horizontal dotted line). We provide experimental confirmation of this characteristic oscillation in Fig. 6B, which shows a representative recording of spontaneous sawtooth-shaped oscillations in perceval-HR from islets exposed to 11 mM glucose (tracing shown was representative of more than 40 islets from 10 mice). As in the model simulation, the mean values of perceval-HR observed during the active and silent phases were very close to the overall mean (Fig. 6B, horizontal dotted line).

Discussion

In the present study, we have addressed the question of whether the main source of the ATP that regulates K_{ATP} activity is oxidative phosphorylation in the mitochondria or glycolysis in a cytosolic compartment in close proximity to K_{ATP} . The context for this question is specifically the oscillations in K_{ATP} conductance that underlie the oscillations in cytosolic calcium, which in turn drive oscillations in insulin secretion (Marinelli et al., 2022; Merrins et al., 2016; Zhang et al., 2020).

Mitochondria produce the vast majority of the ATP in the cell as a whole and inhibition of mitochondrial metabolism completely abolishes calcium oscillations and insulin secretion (Wiederkehr & Wollheim, 2008). After being taken up by beta cells, glucose is metabolized by glycolysis and mitochondrial OxPhos, leading to a large rise in $[ATP]/[ADP]$. According to the consensus model, this increase in $[ATP]/[ADP]$ causes closure of K_{ATP} , which depolarizes the plasma membrane and in turn activates voltage-gated calcium channels. The increase in intracellular free calcium that results triggers the exocytosis of insulin from beta cells (Corkey et al., 1988; Klec et al., 2019). However, this model has been challenged recently (Foster et al., 2022; Lewandowski et al., 2020; Merrins et al., 2022) based on two main lines of evidence. First, it was demonstrated that application of PEP and ADP to excised patches could close K_{ATP} , indicating that glycolysis in principle can mediate this function. Second, it was argued that OxPhos turns off when the ADP concentration is low during the silent phase of bursting, although there is no direct experimental evidence that confirm this is the case.

We addressed these assertions in turn. To evaluate the hypothesis that local, glycolytically produced ATP closes K_{ATP} rather than mitochondrially derived ATP, we recorded K_{ATP} activity from mouse beta cells and INS-1 832/13 cells. Application of ADP in combination with PEP did not provoke a clear closure of K_{ATP} , in contrast to previous studies (Foster et al., 2022; Lewandowski et al.,

2020). However, we observed that K_{ATP} channels were inhibited by PEP + ADP if pH was not corrected. We then demonstrated that the reduction of pH that results from PEP application is necessary for the inhibition of K_{ATP} observed in excised patches. This is consistent with prior data showing that protons inhibit K_{ATP} activity (Allard et al., 1995; Misler et al., 1989; Proks et al., 1994; Xu et al., 2001).

It was not indicated in previous studies (Foster et al., 2022; Lewandowski et al., 2020) whether or not the pH was controlled, although a more recent paper from the same group (Ho et al., 2023) states that they rebalanced pH after PEP was added. It is therefore difficult to account for the differences between our results and these others. Based on the experiments that we have conducted, all we can say is that we were unable to reproduce their results using standard methods for assessing channel function by the patch clamp technique. More importantly, even if the conclusions of previous studies (Foster et al., 2022; Ho et al., 2023; Lewandowski et al., 2020) suggesting that glycolytic enzymes are co-localized with K_{ATP} and can generate sufficient ATP to close the channels are correct, local glycolytic activity in those studies was not demonstrated to be required to close K_{ATP} in intact beta cells. *In situ*, the much larger ATP production by mitochondria may dominate.

We therefore made cell-attached patch recordings using 2.8 or 20 mM glucose in the bathing solutions rather than using PEP as fuel. We observed that K_{ATP} activity was little affected by exposing the cells to a PK activator or inhibitor (PKa and PKi, respectively). The ability of these compounds to cross the beta cell plasma membrane was confirmed in separate studies (data not shown). By contrast, perfusion of NaN_3 or rotenone immediately and robustly increased K_{ATP} activity. We consider these results to be incompatible with the hypothesis that K_{ATP} are primarily closed by ATP locally produced by PK action.

In a final set of experiments, we tested the recent claims that OxPhos is incapable of causing the K_{ATP} channel closure that ends each silent phase and initiates the next active phase of bursting because ADP is too low at that time (Foster et al., 2022; Lewandowski et al., 2020; Merrins et al., 2022). We note that this is probably untrue because measurements of $[ATP]/[ADP]$ (Lewandowski et al., 2020; Li et al., 2013; Merrins et al., 2016) show that $[ATP]/[ADP]$ rises during the silent phase and declines during the active phase in a sawtooth pattern. Consequently, mean $[ATP]/[ADP]$ is the same during the active and silent phases, as shown quantitatively in Fig. 5. Therefore, if ADP is too low during the silent phase, it would have to be too low during the active phase as well. Lewandowski et al. (2020) suggested a way around this by arguing that OxPhos is reactivated during the active phase because the calcium increase that occurs during that time activates calcium pumps, thereby raising ADP.

This too is improbable because OxPhos turns on fully at the beginning of the active phase, long before ADP has risen appreciably (Lewandowski et al., 2020; Merrins et al., 2022). The one system parameter that undergoes a rapid change from the beginning of the active phase is cytosolic calcium, which plausibly activates OxPhos through mitochondrial dehydrogenases.

We therefore tested the hypothesis that OxPhos is shut down during the silent phase, focusing on the modulatory effects of calcium by raising and lowering calcium with KCl in the presence of diazoxide to suppress the endogenous oscillations of metabolism. These experiments (Fig. 5B) decisively refuted the hypothesis because $[ATP]/[ADP]$ readily recovered from its nadir when calcium was low, unless OxPhos was blocked with azide or rotenone, in which case $[ATP]/[ADP]$ dropped below the nadir reached during the low calcium phase. The drop below nadir provides independent evidence that OxPhos was active during the silent phase of a burst even when its substrate ADP was low.

The above considerations are succinctly captured by the IOM mathematical model for islet calcium oscillations (Figs. 5A and 6A). The model shows that ADP does fall during the silent phase, but not very much, and predicts that ATP production continues throughout the silent phase at only a slightly reduced level. Finally, the representative trace of $[ATP]/[ADP]$ shown in Fig. 6B conforms to many other experimental recordings of the $[ATP]/[ADP]$ ratio using perceval-HR. All show the same sawtooth-shaped oscillations predicted by the model (Lewandowski et al., 2020; Li et al., 2013; Merrins et al., 2016).

Taken together, our results support mitochondria as the physiologically important source of ATP in beta cells, as predicted by the IOM model, and also raise questions about the reproducibility of the previous study (Lewandowski et al., 2020) suggesting that PK plays a central role in K_{ATP} regulation in these cells.

References

- Allard, B., Lazdunski, M., Rougier, O. (1995). Activation of ATP-dependent K^+ channels by metabolic poisoning in adult mouse skeletal muscle: Role of intracellular Mg^{2+} and pH. *The Journal of Physiology*, **485**(2), 283–296.
- Anastasiou, D., Yu, Y., Israelsen, W. J., Jiang, J.-K., Boxer, M. B., Hong, B. S., Tempel, W., Dimov, S., Shen, M., Jha, A., Yang, H., Mattaini, K. R., Metallo, C. M., Fiske, B. P., Courtney, K. D., Malstrom, S., Khan, T. M., Kung, C., Skoumbourdis, A. P., ... Vander Heiden, M. G. (2012). Pyruvate kinase M2 activators promote tetramer formation and suppress tumorigenesis. *Nature Chemical Biology*, **8**(10), 839–847.
- Ashcroft, F. M., Harrison, D. E., & Ashcroft, S. J. H. (1984). Glucose induces closure of single potassium channels in isolated rat pancreatic beta-cells. *Nature*, **312**(5993), 446–448.
- Ashcroft, F. M., Puljung, M. C., & Vedovato, N. (2017). Neonatal diabetes and the K_{ATP} Channel: From mutation to therapy. *Trends in Endocrinology and Metabolism*, **28**(5), 377–387.
- Ashcroft, F. M., & Rorsman, P. (1989). Electrophysiology of the pancreatic beta-cell. *Progress in Biophysics and Molecular Biology*, **54**(2), 87–143.
- Bertram, R., Satin, L. S., & Sherman, A. S. (2018). Closing in on the mechanisms of pulsatile insulin secretion. *Diabetes*, **67**(3), 351–359.
- Bokvist, K., Ammala, C., Ashcroft, F. M., Berggren, P. O., Larsson, O., & Rorsman, P. (1991). Separate processes mediate nucleotide-induced inhibition and stimulation of the ATP-regulated K^+ -channels in mouse pancreatic β -cells. *Proceedings of the Royal Society B: Biological Sciences*, **243**, 139–144.
- Chan, K., Truong, D., Shangari, N., & O'Brien, P. J. (2005). Drug-induced mitochondrial toxicity. *Expert Opinion on Drug Metabolism & Toxicology*, **1**(4), 655–669.
- Cook, D. L., & Hales, N. (1984). Intracellular ATP directly blocks K^+ channels in pancreatic B-cells. *Nature*, **311**(5983), 271–273.
- Corkey, B. E., Tornheim, K., Deeney, J. T., Glennon, M. C., Parker, J. C., Matschinsky, F. M., Ruderman, N. B., & Prentki, M. (1988). Linked oscillations of free Ca^{2+} and the ATP/ADP ratio in permeabilized RINm5F insulinoma cells supplemented with a glycolyzing cell-free muscle extract. *Journal of Biological Chemistry*, **263**(9), 4254–4258.
- Digrucchio, M. R., Mawla, A. M., Donaldson, C. J., Noguchi, G. M., Vaughan, J., Cowing-Zitron, C., Van Der Meulen, T., & Huising, M. O. (2016). Comprehensive alpha, beta and delta cell transcriptomes reveal that ghrelin selectively activates delta cells and promotes somatostatin release from pancreatic islets. *Molecular Metabolism*, **5**(7), 449–458.
- Fan, Z., Tokuyama, Y., & Makielski, J. C. (1994). Modulation of ATP-sensitive K^+ channels by internal acidification in insulin-secreting cells. *American Journal of Physiology*, **267**(4), C1036–C1044.
- Foster, H. R., Ho, T., Potapenko, E., Sdao, S. M., Huang, S. M., Lewandowski, S. L., Vandeuken, H. R., Davidson, S. M., Cardone, R. L., Prentki, M., Kibbey, R. G., & Merrins, M. J. (2022). β -cell deletion of the PKm1 and PKm2 isoforms of pyruvate kinase in mice reveals their essential role as nutrient sensors for the K_{ATP} channel. *Elife*, **11**, e79422.
- Ho, T., Potapenko, E., Davis, D. B., & Merrins, M. J. (2023). A plasma membrane-associated glycolytic metabolon is functionally coupled to K_{ATP} channels in pancreatic α and β cells from humans and mice. *Cell Reports*, **42**(4), 112394.
- Kaufman, B. A., Li, C., & Soleimanpour, S. A. (2015). Mitochondrial regulation of β -cell function: Maintaining the momentum for insulin release. *Molecular Aspects of Medicine*, **42**, 91–104.
- Klec, C., Ziomek, G., Pichler, M., Malli, R., & Graier, W. F. (2019). Calcium signaling in β -cell physiology and pathology: A revisit. *International Journal of Molecular Sciences*, **20**(24), 6110.
- Larsson, O., Kindmark, H., Brandstrom, R., Fredholm, B., & Berggren, P. O. (1996). Oscillations in K_{ATP} channel activity promote oscillations in cytoplasmic free Ca^{2+} concentration in the pancreatic beta cell. *The Proceedings of the National Academy of Sciences*, **93**(10), 5161–5165.

- Lewandowski, S. L., Cardone, R. L., Foster, H. R., Ho, T., Potapenko, E., Poudel, C., VanDeusen, H. R., Sdao, S. M., Alves, T. C., Zhao, X., Capozzi, M. E., de Souza, A. H., Jahan, I., Thomas, C. J., Nunemaker, C. S., Davis, D. B., Campbell, J. E., Kibbey, R. G. & Merrins, M. J. (2020). Pyruvate kinase controls signal strength in the insulin secretory pathway. *Cell Metabolism*, **32**, 736–750.e5.
- Li, J., Shuai, H. Y., Gylfe, E., & Tengholm, A. (2013). Oscillations of sub-membrane ATP in glucose-stimulated beta cells depend on negative feedback from Ca^{2+} . *Diabetologia*, **56**(7), 1577–1586.
- Marinelli, I., Fletcher, P. A., Sherman, A. S., Satin, L. S., & Bertram, R. (2021). Symbiosis of electrical and metabolic oscillations in pancreatic β -cells. *Frontiers in Physiology*, **12**, <https://doi.org/10.3389/fphys.2021.781581>.
- Marinelli, I., Thompson, B. M., Parekh, V. S., Fletcher, P. A., Gerardo-Giorda, L., Sherman, A. S., Satin, L. S., & Bertram, R. (2022). Oscillations in K_{ATP} conductance drive slow calcium oscillations in pancreatic β -cells. *Biophysical Journal*, **121**(8), 1449–1464.
- Merrins, M. J., Corkey, B. E., Kibbey, R. G., & Prentki, M. (2022). Metabolic cycles and signals for insulin secretion. *Cell Metabolism*, **34**(7), 947–968.
- Merrins, M. J., Poudel, C., Mckenna, J. P., Ha, J., Sherman, A., Bertram, R., & Satin, L. S. (2016). Phase analysis of metabolic oscillations and membrane potential in pancreatic islet β -cells. *Biophysical Journal*, **110**(3), 691–699.
- Misler, S., Gillis, K., & Tabcharani, J. (1989). Modulation of gating of a metabolically regulated, ATP-dependent K^+ channel by intracellular pH in β cells of the pancreatic islet. *Journal of Membrane Biology*, **109**(2), 135–143.
- Mitok, K. A., Freiberger, E. C., Schueler, K. L., Rabaglia, M. E., Stapleton, D. S., Kwiecien, N. W., Malec, P. A., Hebert, A. S., Broman, A. T., Kennedy, R. T., Keller, M. P., Coon, J. J., & Attie, A. D. (2018). Islet proteomics reveals genetic variation in dopamine production resulting in altered insulin secretion. *Journal of Biological Chemistry*, **293**(16), 5860–5877.
- Nichols, C. G. (2006). K_{ATP} channels as molecular sensors of cellular metabolism. *Nature*, **440**(7083), 470–476.
- Ning, X., Qi, H., Li, R., Li, Y., Jin, Y., McNutt, M. A., Liu, J., & Yin, Y. (2017). Discovery of novel naphthoquinone derivatives as inhibitors of the tumor cell specific M2 isoform of pyruvate kinase. *European Journal of Medicinal Chemistry*, **138**, 343–352.
- Pipatpolkai, T., Usher, S., Stansfeld, P. J., & Ashcroft, F. M. (2020). New insights into K_{ATP} channel gene mutations and neonatal diabetes mellitus. *Nature Reviews Endocrinology*, **16**(7), 378–393.
- Prakasam, G., & Bamezai, R. N. K. (2018). Pyruvate kinase. In *Encyclopedia of Cancer*, pp. 311–320. Elsevier.
- Proks, P., Takano, M., & Ashcroft, F. M. (1994). Effects of intracellular pH on ATP-sensitive K^+ channels in mouse pancreatic beta-cells. *The Journal of Physiology*, **475**(1), 33–44.
- Rorsman, P., & Ashcroft, F. M. (2018). Pancreatic β -cell electrical activity and insulin secretion: Of mice and men. *Physiological Reviews*, **98**(1), 117–214.
- Rorsman, P., & Trube, G. (1985). Glucose dependent K^+ -channels in pancreatic beta-cells are regulated by intracellular ATP. *Pflugers Archiv: European Journal of Physiology*, **405**(4), 305–309.
- Rutter, G. A., Sidarala, V., Kaufman, B. A., & Soleimanpour, S. A. (2023). Mitochondrial metabolism and dynamics in pancreatic beta cell glucose sensing. *Biochemical Journal*, **480**(11), 773–789.
- Satin, L. S., Butler, P. C., Ha, J., & Sherman, A. S. (2015). Pulsatile insulin secretion, impaired glucose tolerance and type 2 diabetes. *Molecular Aspects of Medicine*, **42**, 61–77.
- Tantama, M., Martínez-François, J. R., Mongeon, R., & Yellen, G. (2013). Imaging energy status in live cells with a fluorescent biosensor of the intracellular ATP-to-ADP ratio. *Nature Communications*, **4**(1), 2550.
- Wang, Z., Gurlo, T., Matveyenko, A. V., Elashoff, D., Wang, P., Rosenberger, M., Junge, J. A., Stevens, R. C., White, K. L., Fraser, S. E., & Butler, P. C. (2021). Live-cell imaging of glucose-induced metabolic coupling of β and α cell metabolism in health and type 2 diabetes. *Communications Biology*, **4**(1), 594.
- Wiederkehr, A., & Wollheim, C. (2008). Impact of mitochondrial calcium on the coupling of metabolism to insulin secretion in the pancreatic beta-cell. *Cell Calcium*, **44**(1), 64–76.
- Xu, H., Wu, J., Cui, N., Abdulkadir, L., Wang, R., Mao, J., Giwa, L. R., Chanchevalap, S., & Jiang, C. (2001). Distinct histidine residues control the acid-induced activation and inhibition of the cloned K_{ATP} channel. *Journal of Biological Chemistry*, **276**(42), 38690–38696.
- Yakubovich, D., Rishal, I., Dessauer, C. W., & Dascal, N. (2009). Amplitude histogram-based method of analysis of patch clamp recordings that involve extreme changes in channel activity levels. *Journal of Molecular Neuroscience*, **37**(3), 201–211.
- Zhang, I. X., Ren, J., Vadrevu, S., Raghavan, M., & Satin, L. S. (2020). ER stress increases store-operated Ca^{2+} entry (SOCE) and augments basal insulin secretion in pancreatic beta cells. *Journal of Biological Chemistry*, **295**(17), 5685–5700.
- Zhang, Z., Deng, X., Liu, Y., Liu, Y., Sun, L., & Chen, F. (2019). PKM2, function and expression and regulation. *Cell Biosciences*, **9**(1), 52.

Additional information

Data availability statement

Data are available from the corresponding author upon reasonable request.

Competing interests

The authors declare that they have no competing interests.

Author contributions

J.C. and B.T. performed experiments and analysed data. P.A.F. performed model simulations. R.B., A.S.S. and L.S.S. provided supervision and resources. All authors contributed to writing the paper.

Funding

This research was supported by the National Institute of Diabetes and Digestive and Kidney Diseases grants RO1 DK46409 and U01 DK127747-01 (to LSS). RB was partially supported by grant number DMS 2 324 962 from the National Science Foundation. PAF and ASS were supported by the Intramural Research Program of the National Institute of Diabetes and Digestive and Kidney Diseases (NIH) under ZIA DK013027-16.

Acknowledgements

We thank Chanté Liu for contributing the data shown in Fig. 6B and for her help isolating islets.

Keywords

[ATP]/[ADP] ratio, beta cells, glucose response, insulin secretion, K_{ATP} channels, oxidative phosphorylation, pH modulation, pyruvate kinase

Supporting information

Additional supporting information can be found online in the Supporting Information section at the end of the HTML view of the article. Supporting information files available:

Statistical Summary Document

Peer Review History

Supplementary Materials